
Inflammatory Flux and Disease Progression in Hidradenitis Suppurativa: A Multi-Compartment Deterministic Model Simulating Lifestyle and Pharmaceutical Interventions in In Silico Cohorts

[Jaap-Jan Roukens](#)*

Posted Date: 2 March 2026

doi: 10.20944/preprints202603.0022.v1

Keywords: hidradenitis suppurativa; mathematical modeling; In Silico clinical trials; systems biology; pharmacokinetics; biologics; antibiotics; corticosteroids; inflammatory flux; lesion hysteresis; lifestyle



Preprints.org is a free multidisciplinary platform providing preprint service that is dedicated to making early versions of research outputs permanently available and citable. Preprints posted at Preprints.org appear in Web of Science, Crossref, Google Scholar, Scilit, Europe PMC.

Copyright: This open access article is published under a [Creative Commons CC BY 4.0 license](#), which permit the free download, distribution, and reuse, provided that the author and preprint are cited in any reuse.

Disclaimer/Publisher's Note: The statements, opinions, and data contained in all publications are solely those of the individual author(s) and contributor(s) and not of MDPI and/or the editor(s). MDPI and/or the editor(s) disclaim responsibility for any injury to people or property resulting from any ideas, methods, instructions, or products referred to in the content.

Article

Inflammatory Flux and Disease Progression in Hidradenitis Suppurativa: A Multi-Compartment Deterministic Model Simulating Lifestyle and Pharmaceutical Interventions in In Silico Cohorts

Jaap-Jan Roukens

Independent Scientist & R&D Consultant, 3014 Bern, Switzerland; jaapjanroukens@gmail.com

Abstract

While recent reviews have firmly established hidradenitis suppurativa (HS) as a systemic inflammatory disorder inextricably linked to metabolic comorbidities, the investigation of lifestyle determinants remains a fraction of the research effort compared to the pursuit of pharmaceuticals. Consequently, current clinical approaches may not fully leverage natural modulators of systemic environmental inflammatory influx, a potential driver of the disease. The central premise of this study posits that the compromise of follicular integrity is directly coupled to lifestyle-driven systemic inflammation exceeding a critical threshold. While previous studies have relied on statistical regression and probabilistic frameworks for HS, this study establishes a deterministic multi-compartment ordinary differential equation framework to simulate the longitudinal kinetics of systemic and local lesion inflammation. Represented in this framework is the first mathematical formalization of the 2025 European S2k guideline interventions, explicitly modeling the resistance kinetics of antibiotics, the immunogenic decay of biologics, and the tapering dynamics of corticosteroids to simulate their longitudinal efficacy in HS. Furthermore, we introduce an abstractified framework that applies the laws of mass balance and pharmacokinetics directly to the disease state and key biologically relevant parameters, rather than focusing on cell types, targets, and individual cytokines. In this HS PK model, the lesion is connected to the systemic inflammation and acts as an integrator and amplifier, recording transient systemic spikes as permanent structural debt through an effect of hysteresis that progressively decouples the lesion from the systemic driver. Simulation studies suggest biologic agents provide a buffering capacity that creates a therapeutic equilibrium, which differs from resolving the underlying inflammatory mass balance. When evaluated across a virtual cohort, this reveals distinct kinetic populations. We demonstrate that clinical rebound is mathematically governed by phase space topology, where the disease state acts as a stable natural equilibrium. Upon pharmaceutical cessation, the therapeutic equilibrium collapses, causing the system to shift rapidly back to the disease state, driven by the underlying inflammatory load. Consequently, a comparative rescue trial demonstrated that pharmacological escalation encounters a saturation ceiling. This suggests that sustainable remission in HS may require a transformation that shifts the equilibrium itself, redefining lifestyle modification from an adjuvant option to the fundamental variable required to treat HS effectively.

Keywords: hidradenitis suppurativa; mathematical modeling; In Silico clinical trials; systems biology; pharmacokinetics; biologics; antibiotics; corticosteroids; inflammatory flux; lesion hysteresis; lifestyle

1. Introduction

1.1. *The Stochastic Limitation: Re-Evaluating Therapeutic Failure in HS*

Current therapeutic models for hidradenitis suppurativa (HS) rely predominantly on the suppression of single pathway cytokines such as TNF alpha and IL 17. These approaches reflect the stochastic perception of the disease as a probabilistic failure of the immune system where flares are treated as independent events triggered by unpredictable variables. Consequently, current clinical models may not fully account for the high variance in remission rates and the phenomenon of secondary failure where pharmaceuticals lose efficacy over time due to antidrug antibody formation or pathway compensation [1].

A recent landmark review defines HS not merely as a cutaneous inflammatory condition but as a systemic inflammatory pathology linked to metabolic syndrome, insulin resistance, central obesity and other inflammatory conditions [2]. Crucially these comorbidities are not merely collateral damage but share the same inflammatory mediators that drive the cutaneous pathology. This suggests a causal feedback loop where systemic metabolic dysfunction acts as a continuous systemic inflammatory input flux driving the disease from the inside out. This hypothesis is supported by the concept of a window of opportunity [3] which posits that early intervention can prevent the irreversible formation of draining tunnels implying a deterministic time-dependent progression rather than a random series of flares.

Furthermore the observed clinical trajectory indicates that the hair follicle is structurally coupled to this systemic inflammatory load acting as a localized integrator of lifestyle. The transition from reversible inflammation to irreversible tunneling follows a defined timeline rather than a random pattern. Therefore, the stochastic paradigm framing the disease as random events may warrant re-evaluation.

1.2. *The Misclassification of Lifestyle Adjuvants*

The newly released 2025 European S2k Guidelines represent a significant advancement in the pharmaceutical and surgical management of Hidradenitis Suppurativa but simultaneously illustrate the limitations of the current paradigm [4]. While the guidelines explicitly categorize weight reduction and smoking cessation as adjuvant treatments, they conclude that evidence for specific dietary interventions is insufficient for a stronger recommendation. This conclusion, while adhering to the strict hierarchy of evidence-based medicine, presents a clinical inconsistency: the guidelines acknowledge the strong association between metabolic dysfunction and HS yet systematically deprioritize the interventions most capable of correcting this dysfunction.

Given that systemic inflammation is the key driver of this disease and that diet and lifestyle are the primary regulators of inflammatory load. The classification of these factors primarily as adjuvants may limit the therapeutic scope regarding upstream drivers of inflammatory flux. This strict reliance on randomized controlled trial (RCT) data causes the actual primary upstream drivers of inflammatory flux and HS disease genesis and progression to be systematically undervalued in the HS literature. Consequently, when these pharmaceuticals are removed without correcting the baseline flux of systemic inflammation, patients inevitably experience the rebound effect and progressive disease recurrence. This trajectory is often mistaken for the natural course of the disorder rather than a failure of containment.

To operationalize this critique, the present study introduces a computational framework capable of simulating the longitudinal dynamics of biologically relevant parameters on both systemic and local lesion inflammation. By mathematically integrating novel efficacy equations for the systemic administration of antibiotics, biologics, and corticosteroids, this pharmacokinetic model isolates the specific impact of lifestyle versus pharmaceutical suppression on HS lesion activity. This approach allows for a quantitative reconstruction of the interaction between patient variability in lifestyle, therapeutic interventions, and disease progression, transforming the abstract concept of treatment failure into a solvable equation.

1.3. *Mathematical Novelty and Convergence with Autoimmune Pathologies*

The literature currently possesses no deterministic mathematical description of hidradenitis suppurativa. While quantitative systems pharmacology (QSP) successfully models psoriasis and rheumatoid arthritis through kinetic principles [5–8], the study of hidradenitis suppurativa remains confined to probabilistic frameworks and statistical regression [9–12]. This study introduces a deterministic model that differentiates itself from standard computational immunology by focusing on disease state and key parameters of the disease itself instead of focusing on cells, targets and individual cytokines. By abstracting the principles of pharmacokinetics and mass balance, we bypass the granular Michaelis-Menten kinetics of drug-target binding, which are often mathematically incompatible with broad environmental variables.

This abstraction allows for the integration of lifestyle factors and pharmaceutical interventions into a single unified framework. The validity of this approach rests on the premise that, when viewed macroscopically, these disparate parameters share a common denominator: they all functionally modulate the systemic inflammatory concentration. This transformation models the disease state as a dynamic flow governed by the aggregate rate of elimination, where clinical phenomena emerge as mathematical consequences of mass balance rather than programmed rules. The quantification of inflammation in arbitrary inflammatory units (AIU) represents a necessary theoretical abstraction to facilitate this kinetic analysis. This simplification aggregates the functional concentration of diverse inflammatory mediators into a single variable to allow for the calculation of clearance. We further introduce a coupling coefficient and a structural hysteresis term to quantify the decoupling of the damaged tissue. This inclusion provides a mathematical explanation for the autonomous persistence of established HS lesions despite systemic improvement which offers a distinct advancement over receptor saturation models.

1.4. *Novel Pharmacological Efficacy Equations and the in Silico Clinical Trial Framework.*

Beyond the disease topology, this study proposes a mathematical formalism for the pharmaceutical and surgical interventions recommended by the 2025 European S2k guidelines [4]. Standard pharmacokinetic models often rely on static parameters such as minimum inhibitory concentrations or equilibrium binding constants, which fail to capture the functional decay of efficacy observed in long-term clinical practice. To address this limitation, we apply an indirect response modeling framework to simulate therapeutic modalities not as constant effects but as time-dependent covariates of efficacy.

For systemic antibiotics, we utilize a resistance state variable to quantify the adaptive evolution of the microbiome. This differential equation simulates resistance acquisition during exposure and decay during cessation, effectively modeling the antimicrobial agent as a depleting resource rather than a constant suppressor. Similarly, for biologic therapies, we model the loss of response using a hazard function calibrated to represent immunogenic decay. This approach treats the biologic agent as a functional unit subject to probability of failure, which allows for the prediction of secondary non-response rates and the emergence of antidrug antibodies over time.

To accurately represent the multi-modal approach emphasized by the guidelines, we define the model as a hybrid dynamical system. This formalism allows for the integration of continuous differential equations governing inflammatory flux with discrete event simulations representing physical interventions. Intralesional corticosteroid injections are modeled as a linear superposition of impulse responses, where the cumulative anti-inflammatory pressure of multiple depot injections is summed to simulate the localized resolution of nodules. Surgical intervention is modeled as a discrete state reset event, where the local lesion topology and structural hysteresis undergo an instantaneous reduction to zero at the moment of excision. This hybrid framework enables the performance of virtual clinical trials to predict not merely the immediate efficacy of an intervention, but its long-term durability against the inevitable forces of resistance and homeostatic rebound.

1.5. Integrating Environmental Determinants: Bridging the Gap in Current Computational Immunology

A critical review of the current state of the art in autoimmune modeling reveals a significant methodological gap defined by the systemic exclusion of lifestyle and environmental factors as variable inputs. While sophisticated QSP models exist for rheumatoid arthritis and psoriasis they are almost exclusively drug centric. These frameworks typically model the interaction between a therapeutic molecule and its target with high fidelity but they treat the baseline inflammatory state of the patient as a static constant or a stochastic noise variable.

Approaches that do not explicitly model lifestyle factors may not account for the dynamic daily fluctuation of inflammatory drivers. Current literature acknowledges that factors such as antigenicity [13], glycemic load [14], chronic psychological stress [15] and circadian immune modulation [16] are potent mediators of the very cytokine pathways these drugs attempt to modulate. By omitting these variables standard models inevitably overestimate the long-term efficacy of pharmaceutical monotherapy and fail to predict secondary non-response in patients with high metabolic or psychosocial burden.

This HS PK model addresses this limitation by explicitly parameterizing these invisible drivers. We integrate dietary antigen intake, gut permeability and stress inputs not as optional quality of life metrics but as fundamental kinetic forces that directly oppose therapeutic clearance. This topological inclusion explains why two patients with identical genetic biomarkers may have vastly different therapeutic outcomes. One patient exhibits a net inflammatory velocity where the clearance capacity exceeds the input flux while the other exhibits a state where the lifestyle flux exceeds the maximum stoichiometric clearance of the drug. By mathematically quantifying these inputs, we aim to move toward a deterministic understanding of therapeutic non-response.

2. Methods: The Mathematical Framework

2.1. The Multi-Compartment Network

We model hidradenitis suppurativa as a coupled system consisting of two distinct compartments: the systemic inflammatory state (C_{SI}), which represents the cumulative load of circulating mediators, and the local inflammatory state of a specific lesion (C_{LI}).

Equation 1: Systemic inflammatory state (C_{SI})

The global inflammatory potential is defined as a mass balance of net flux multiplied by genetic susceptibility, minus total clearance.

$$\frac{dC_{SI}}{dt} = J_{in} - (k_{clear}(t) * C_{SI}) \quad (1)$$

J_{in} : (Net inflammatory influx): The aggregate inflammatory input derived from diet, stress, and permeability, multiplied by genetic gain. $k_{input} = \phi_{net} * \sigma_{gen}$

σ_{gen} (Genetic and epigenetic gain): A scalar multiplier representing innate immune reactivity (e.g., notch/gamma-secretase pathways). A healthy control has a low gain (approx 0.2), while an HS patient has a high gain (greater than or equal to 1.0).

k_{clear} : Net inflammatory efflux, which is the sum of genetic basal capacity (k_{basal}), active lifestyle modulation (k_{life}) and pharmaceutical intervention (k_{pharma}).

The fundamental dynamics of the system are governed by the differential mass balance defined in Equation 1. For intervals of constant input and clearance, this yields the analytical solution described in Equation 2. However, to accurately capture the continuous time-dependent fluctuations of drug tapering and lifestyle variability used in this simulation, the full differential system (Equation 1) was solved numerically (see Section 2.5).

$$C_{SI}(t) = \frac{J_{in}}{k_{clear}} \cdot (1 - e^{-k_{clear} \cdot t}) + C_{initial} \cdot e^{-k_{clear} \cdot t} \quad (2)$$

Equation 2: Local inflammatory state

Established lesions exhibit autonomous dynamics that often persist despite systemic remission. The activity of a specific lesion is governed by a decoupled differential equation:

$$\frac{dC_{LI}}{dt} = (\beta * C_{SI}(t)) + k_{auto}(t) - (k_{resolve} * C_{LI}) \quad (3)$$

$k_{resolve}$: The local resolution rate.

β : The transfer rate constant, a scalar (0 to 1) defining the lesion's connectivity to systemic blood flow. In chronic damaged tissue, β approaches 0, rendering the lesion decoupled from the systemic inflammatory state (C_{SI}).

$k_{auto}(t)$: The time-dependent autoinflammatory drive generated by the structural hysteresis of the damaged tissue (H).

Crucially H , is defined as a slow-manifold state variable representing the physical accumulation of damaged skin tissue (abscesses, epithelialized dermal tunnels, enlarged epidermis, infiltration of immune cells, etc.). Unlike the fast kinetics of inflammatory hormones, this structural pathology evolves according to:

$$\frac{dH}{dt} = (k_{dam} \cdot C_{LI}(t)) - (k_{remodel} \cdot H(t)) \quad (3a)$$

Here, k_{dam} represents the rate of tissue damage accumulation driven by local inflammation, while $k_{remodel}$ defines the slow rate of physiological tissue remodeling and healing. The resulting inflammatory feedback is explicitly defined by the coupling equation:

$$k_{auto}(t) = k_{foreign} \cdot H(t) \quad (3b)$$

The model assumes the body treats the damaged skin as a foreign object. $k_{foreign}$ represents how strongly the immune system reacts to that specific amount of scar tissue.

This system of equations (3–3b) mathematically separates the fast kinetics of inflammatory mediators from the slow kinetics of tissue remodeling. It ensures that short-term pharmaceutical suppression of C_{LI} does not immediately eliminate the structural driver H .

Net environmental flux (J_{net}): This value represents the raw input before genetic amplification.

$$\phi_{net} = J_{diet} \cdot (1 + \gamma_{gut}) + J_{stress} + J_{sleep} \quad (4)$$

J_{diet} : Allergens

γ_{gut} : Intestinal permeability multiplier

J_{stress} : Stress

J_{sleep} : Sleep

Note: The permeability acts as a scalar multiplier. If gut integrity is compromised ($\gamma_{gut} > 0$), the impact of antigenic flux (A) is amplified.

To integrate the clearance terms the total systemic clearance (K_{clear}) is defined as:

$$k_{clear} = k_{basal} + k_{lifestyle} + k_{pharma} \quad (5)$$

where k_{basal} is genetic and epigenetic basal capacity, $k_{lifestyle}$ is lifestyle modulation, and k_{pharma} is pharmaceutical suppression.

2.2. Novel Equations to Model Steroids, Biologicals and Antibiotics in Hidradenitis Suppurativa

2.2.1. Systemic Antibiotic Resistance

The European S2k guidelines [4] recommend systemic antibiotics (e.g., tetracyclines, clindamycin-rifampicin) as first-line therapy for inflammatory HS, typically administered for 12-week courses. As described, the long-term exposure carries the risk of inducing antimicrobial resistance (AMR) within the cutaneous microbiome. To simulate the time-dependent loss of efficacy often observed in clinical practice, we introduce the dimensionless resistance state variable (S_{res}).

Unlike population-genetic models that track individual bacterial strains, this scalar variable represents the aggregate adaptive resistance of the microbiome. The evolution of resistance is governed by a learning-forgetting dynamic:

$$\frac{dS_{res}}{dt} = k_{learn} \cdot \mathbb{I}(t \in T_{therapy}) - k_{forget} \cdot S_{res}(t) \quad (6)$$

$$k_{abx}(t) = E_{potency} \cdot e^{-\alpha_{res} S_{res}(t)} \cdot \mathbb{I}(t \leq T_{end}) \quad (6b)$$

Equation 6 describes the acquisition of resistance during the active treatment window. Whenever the patient is actively taking the drug ($t \in T_{therapy}$), the resistance state accumulates at the rate k_{learn} , mathematically representing the selection pressure favoring resistant colonisation. This accumulation is continuously opposed by the elimination rate k_{forget} , which represents the gradual repopulation of the microbiome by wild-type, susceptible flora once the selection pressure is removed.

Equation 6b models the effective pharmacological clearance rate k_{abx} . The intrinsic potency of the antibiotic is defined by the maximum clearance coefficient $E_{potency}$. However, this potency is exponentially attenuated by the current resistance state S_{res} , scaled by the resistance sensitivity coefficient α_{res} . The final term involves the indicator function $\mathbb{I}(t \leq T_{end})$, which acts as a binary switch: it ensures that the drug effect is only non-zero while the simulation time is prior to the therapy cessation time T_{end} . This formulation allows the model to simulate the clinical reality where a drug is initially effective but loses therapeutic control over time as S_{res} rises, necessitating discontinuation or rotation.

2.2.2. Biologic Immunogenicity (Anti-Drug Antibody Formation)

The European S2k guidelines [4] identify secondary loss of response (LOR) as a critical limitation in the long-term management of HS with biologic agents, noting that efficacy often wanes over time due to immunogenicity and the formation of anti-drug antibodies (ADA). To simulate this clinical phenomenon, we model biologic therapy not as a static clearance rate, but as a dynamic efficacy profile subject to stochastic failure. The effective biologic clearance rate k_{bio} is defined by a kinetic induction function constrained by a survival switch:

$$k_{bio}(t) = (1 - e^{-k_{onset}(t - T_{start})}) \cdot (E_{max} e^{-k_{decay}(t - T_{start})}) \cdot \mathbb{I}(t < T_{fail}) \quad (7)$$

Here, E_{max} represents the steady-state pharmacological efficacy achieved during maintenance therapy, while the term $(1 - e^{-k_{onset}(t - T_{start})})$ models the onset of drug efficacy. This induction term captures the physiological delay between the therapy start time and the attainment of therapeutic serum levels, governed by the therapeutic onset k_{onset} . Simultaneously, the steady-state efficacy is subjected to a continuous exponential decline governed by the rate constant (k_{decay}), representing the gradual, erosion of drug potency over time due to the progressive accumulation of low-titer antidrug antibodies (ADA) or other tolerance mechanisms. The critical innovation in this module is the stochastic failure switch $\mathbb{I}(t < T_{fail})$, where the indicator function ensures that the

drug remains effective only while the simulation time precedes the specific failure time T_{fail} . To physically justify this duration, T_{fail} is drawn for each simulation from a Weibull distribution, a standard reliability model for time-to-event data. This distribution is characterized by a scale parameter $\lambda_{weibull}$, representing the characteristic drug survival time (e.g., median time to LOR), and a shape parameter ε_{shape} , which determines the hazard rate evolution over years of exposure ($T_{fail} \sim \text{Weibull}(\lambda, \varepsilon)$). This formulation allows the model to reproduce the drug efficacy curves observed in longitudinal registries, where efficacy is initially high but subject to sudden drug antibody formation and clearance.

2.2.3. Systemic Corticosteroid Tapering

To manage acute flares or as a bridge to surgery, the S2K guidelines recommend short-term courses of systemic corticosteroids (e.g., prednisolone 0.5–0.7 mg/kg). Corticosteroid therapy typically follows a structured clinical protocol consisting of an induction, a maintenance plateau, and a gradual reduction to prevent adrenal insufficiency. To simulate this regimen without introducing excessive discontinuous inputs, we introduce a phenomenological trapezoidal efficacy function:

$$k_{steroid}(t) = E_{steroid} \cdot \text{Trapezoid}(t, T_{start}, T_{plateau}, T_{taper}) \quad (8)$$

Trapezoid(t)

$$= \begin{cases} 0, & t < T_{start} \\ (t - T_{start})/T_{ramp}, & T_{start} \leq t < T_{start} + T_{ramp} \\ 1, & T_{start} + T_{ramp} \leq t < T_{plateau} \\ 1 - ((t - T_{plateau})/T_{taper}), & T_{plateau} \leq t < T_{plateau} + T_{taper} \\ 0, & t \geq T_{plateau} + T_{taper} \end{cases} \quad (8a)$$

Here, $E_{steroid}$ represents the maximum clearance efficacy achieved during the high-dose plateau. The function describes the temporal shape of the therapy: a linear increase from zero T_{start} at to the maximum dose, a sustained plateau for the duration $T_{plateau}$, and a linear decay to zero over the tapering period T_{taper} . This formulation mathematically abstracts the discrete daily dosing changes into a continuous efficacy envelope, capturing the anti-inflammatory impact of the standard "tapering course" frequently utilized in refractory disease management.

2.2.4. Aggregate Clearance and Surgical Reset

The total systemic pharmacological clearance $k_{pharma}(t)$ is calculated as the superposition of all concurrent interventions. Assuming no direct pharmacokinetic interaction between these distinct drug classes, the aggregate rate is defined as the scalar sum of the biologic, antibiotic, and steroid clearance functions derived in the preceding sections:

$$k_{pharma}(t) = k_{bio}(t) + k_{abx}(t) + k_{steroid}(t) \quad (9)$$

Finally, the guidelines emphasize that for advanced disease (Hurley stage II/III) characterized by irreversible tissue destruction, medical therapy alone is often insufficient and must be combined with surgery. We model surgical intervention not as a continuous rate, but as a discrete state reset event within a hybrid dynamical system. At the moment of surgery $T_{surgery}$, the state variables governing local pathology are instantaneously forced to post-operative baseline values:

$$E_{surgery}: C_{LI} \rightarrow C_{healing}, \quad k_{auto} \rightarrow 0, \quad k_{inject} \rightarrow 0, \quad H \rightarrow 0.1 \quad (10)$$

This impulse control mechanism instantaneously resets the local inflammatory state (C_{LI}) to a baseline healing value ($C_{healing}$). Crucially, the autoinflammatory drive is reset to zero ($k_{auto} \rightarrow$

0), representing the excision of the fistulous tract. Simultaneously, the injection rate is forced to zero ($k_{inject} \rightarrow 0$), ensuring that any active pharmacological depots are physically removed along with the excised tissue. Crucially, the structural hysteresis is reset to a residual baseline ($H \approx 0.1$ AIU), representing the microscopic retention of damaged and scarred tissue or incomplete excision that predisposes the site to future recurrence. This hybrid formulation allows the model to simulate HS, where medical therapy reduces inflammatory load while surgery eliminates the autonomous drivers of severe disease recurrence.

2.2.5. Intralesional Depot Kinetics

Local corticosteroid injections (e.g., triamcinolone acetonide) are modeled using a one-compartment extravascular absorption framework. To ensure clinical validity, the dosing parameters are derived directly from the S2k guidelines [4]. These guidelines explicitly recommend triamcinolone acetonide concentrations of 10–40 mg/mL for the management of recalcitrant nodules and tunnels.

Accordingly, we define the injection event as an adaptive dosing function that scales the active drug mass to the lesion bio-burden. The total intralesional clearance rate $k_{inject}(t)$ is calculated as:

$$V_{inject,k} = \min(V_{max}, \alpha_{dose} \cdot C_{LI}(T_k)) \quad (11)$$

$$k_{inject}(t) = \sum_{k=1}^{N_{shots}} (C_{drug} \cdot V_{inject,k}) \cdot \alpha_{efficacy} \cdot e^{-k_{local}(t-T_k)} \cdot \mathbb{I}(t > T_k) \quad (11a)$$

Equation 11 defines the administered volume $V_{inject,k}$ for the k -th injection event. The injected volume is scaled linearly to the local inflammatory load C_{LI} via the dosing scalar α_{dose} , constrained by a safety ceiling V_{max} . This simulates clinical practice where highly active, inflamed lesions require larger therapeutic volumes compared to less inflamed lesions.

Equation 11a calculates the resulting pharmacological clearance. The total drug mass is the product of the adaptive volume and the drug concentration C_{drug} . This formulation allows the model to simulate the guideline-based heterogeneity in dosing, distinguishing between the standard 10 mg/mL dosage used for inflammatory nodules and the higher 40 mg/mL concentration indicated for recalcitrant tunnels. This mass is converted into an elimination rate via the efficacy coefficient $\alpha_{efficacy}$ and decays exponentially according to the pharmaceutical half-life λ_{local} .

2.3. Notation and Parameter Definitions

Table 1. Mathematical notation and parameter definitions. AIU = Arbitrary Inflammatory Units (dimensionless functional measure) - All time-dependent parameters denoted explicitly with (t) - Dimensionless parameters denoted with [-].

| Symbol | Definition | Units | Equation(s) |
|-------------------------|--|----------|-------------|
| <i>State variables</i> | | | |
| $C_{SI}(t)$ | Systemic inflammatory concentration | AIU | 1, 2 |
| $C_{LI}(t)$ | Local lesion inflammatory concentration | AIU | 3 |
| $S_{res}(t)$ | Antibiotic resistance state | [-] | 6 |
| $H(t)$ | Structural hysteresis of damaged tissue | AIU | 3a, 3b, |
| <i>Input parameters</i> | | | |
| J_{diet} | [Diet] Antigenic load input | AIU/time | 4 |
| γ_{gut} | [Gut] Intestinal permeability multiplier | [-] | 4 |

| | | | |
|----------------------------------|--|-----------------|-------------|
| J_{stress} | [Psych] Stress contribution | AIU/time | 4 |
| J_{sleep} | [Sleep] Circadian disruption contribution | AIU/time | 4 |
| J_{net} | [Total] Net environmental flux (Pre-genetic) | AIU/time | 4 |
| σ_{gen} | [Genetics] Susceptibility gain factor | [-] | 1 |
| $C_{initial}$ | [System] Initial inflammatory state at t=0 | AIU | 2 |
| J_{in} | Systemic inflammatory influx | AIU/time | 1, 2 |
| <i>Clearance rates</i> | | | |
| k_{clear} | Total systemic clearance rate (Sum of all) | 1/time | 1, 5 |
| k_{basal} | [Physio] Genetic basal clearance capacity | 1/time | 5 |
| $k_{lifestyle}$ | [Lifestyle] Active modulation clearance | 1/time | 5 |
| $k_{pharma}(t)$ | [Drugs] Total pharmaceutical clearance | 1/time | 5, 9 |
| $k_{resolve}$ | [Local] Lesion resolution rate | 1/time | 3 |
| $k_{auto}(t)$ | [Local] Autonomous inflammatory drive | AIU/time | 3, 3b |
| <i>Coupling parameters</i> | | | |
| β | Coupling coefficient (0 to 1) | 1/time | 3 |
| $K_{foreign}$ | Foreign body reaction amplification | 1/time | 3b |
| k_{damage} | [Local] Structural damage rate constant | 1/time | 3a |
| $k_{remodel}$ | [Local] Structural remodeling rate | 1/time | 3a |
| <i>Pharmaceutical parameters</i> | | | |
| $k_{inject}(t)$ | [Intralesional Steroid] Clearance rate | 1/time | 11a |
| C_{drug} | [Intralesional Steroid] Concentration | mg/mL | 11a |
| $V_{inject,k}$ | [Intralesional Steroid] Volume of k-th injection | mL | 11 |
| V_{max} | [Intralesional Steroid] Safety volume ceiling | mL | 11 |
| α_{dose} | [Intralesional Steroid] Dosing scalar | mL/AIU | 11 |
| $\alpha_{efficacy}$ | [Intralesional Steroid] Efficacy coefficient | 1 / (mg · time) | 11a |
| k_{local} | [Intralesional Steroid] Depot decay rate | 1/time | 11a |
| $k_{abx}(t)$ | [Antibiotics] Systemic clearance rate | 1/time | 6b, 9 |
| $E_{potency}$ | [Antibiotics] Maximum clearance efficacy | 1/time | 6b |
| α_{res} | [Antibiotics] Resistance sensitivity factor | [-] | 6b |
| k_{learn} | [Antibiotics] Resistance acquisition rate | 1/time | 6 |
| k_{forget} | [Antibiotics] Resistance decay rate | 1/time | 6 |
| $k_{bio}(t)$ | [Biologics] Systemic clearance rate | 1/time | 7, 9 |
| E_{max} | [Biologics] Max steady-state efficacy | 1/time | 7 |
| k_{onset} | [Biologics] Therapeutic onset rate | 1/time | 7 |
| k_{decay} | [Biologics] Gradual efficacy loss (ADA) rate | 1/time | 7 |
| T_{fail} | [Biologics] Stochastic failure time | time | 7 |
| $\lambda_{weibull}$ | [Biologics] Weibull scale parameter | time | Section 2.5 |
| ϵ_{shape} | [Biologics] Weibull shape parameter | [-] | Section 2.5 |
| $k_{steroid}(t)$ | [Systemic Steroid] Oral clearance rate | 1/time | 8, 9 |
| $E_{steroid}$ | [Systemic Steroid] Max efficacy (plateau) | 1/time | 8 |
| $C_{healing}$ | [Surgery] Post-op baseline inflammatory state | AIU | 10 |
| <i>Time parameters</i> | | | |
| T_{start} | [General] Therapy initiation time (Bio/Steroid) | time | 7, 8 |

| | | | |
|-------------------------|--|---------------|---------------|
| T_{end} | [Antibiotics] Therapy cessation time | time | 6b |
| T_k | [Intralesional] Time of k-th injection event | time | 11, 11a |
| T_{ramp} | [Systemic Steroids] Induction duration (ramp-up) | time | 8a |
| $T_{plateau}$ | [Systemic Steroids] Time of taper onset | time | 8, 8a |
| T_{taper} | [Systemic Steroids] Duration of taper phase | time | 8, 8a |
| $T_{surgery}$ | [Surgery] Time of surgical intervention | time | 10 |
| <i>Operators</i> | | | |
| $\mathbb{I}(condition)$ | Indicator function (1 if true, 0 if false) | [-] | 6, 6b, 7, 11a |
| $min(a, b)$ | Minimum of a and b | [context-dep] | 11 |

2.4. Model Assumptions and Limitations

The mathematical framework presented herein relies on specific structural abstractions necessary to render the complex systems biology of HS computationally tractable. These modeling choices introduce limitations that warrant explicit acknowledgment:

A1. Phenomenological calibration of resistance:

The decay of therapeutic efficacy for biologics and antibiotics is modeled using phenomenological probability density functions (Weibull distributions) and abstract resistance indices (S_{res}), rather than mechanistic interactions. Consequently, the model simulates the temporal profile of therapeutic failure without explicitly modeling the underlying molecular dynamics of anti-drug antibody titers or bacterial population genetics.

A2. The open-loop environmental assumption:

Equation (4) defines environmental input flux (J_{in}) as an independent variable driven by diet, stress, and sleep. This formulation represents an open-loop control system and does not currently account for the somatopsychic positive feedback loop, where active disease burden (C_{LI}) generates pain and depressive symptoms that endogenously upregulate the stress flux (J_{stress}). The model therefore likely underestimates the self-perpetuating nature of the disease in patients with severe pain syndromes.

A3. Aggregation of Inflammatory Mediators:

By lumping diverse cytokines (TNF- α , IL-17, IL-1 β) into a single functional variable (AIU), the model prioritizes topological behavior over molecular specificity. While this facilitates the study of general inflammatory accumulation, it precludes the differentiation of drug classes. The current framework includes characterised pharmacological agent and cannot predict differential clinical responses between uncharacterised therapeutics.

A4. Parameter identifiability and over-parameterization:

The model parameters were calibrated heuristically to reproduce clinical phenotypes described in the S2k guidelines rather than via regression against patient-specific longitudinal data. Due to the high number of free parameters relative to the observable states, the model implies a degree of structural non-identifiability, where distinct combinations of input flux and clearance capacity could theoretically produce identical disease trajectories.

2.5. Computational Implementation and Statistical Analysis

All mathematical simulations and deterministic projections were executed using the Python programming language, utilizing the NumPy and SciPy libraries for numerical computation. The system of coupled ordinary differential equations describing systemic and local inflammatory dynamics was solved using the `scipy.integrate.odeint` function. This solver implements the LSODA (Livermore solver for ordinary differential equations) algorithm, which automatically switches between non-stiff (adams) and stiff (backward differentiation formula) methods to maintain stability. To mitigate integration errors associated with discontinuous environmental triggers, such as acute stress events or dietary spikes, the simulation time grid was constructed adaptively. The standard

resolution of 2,000 time points was augmented with explicit boundary points at the initiation and cessation of each trigger event to ensure the precise capture of rapid flux transitions.

To evaluate population-level heterogeneity, a virtual clinical trial cohort of 250 patients was generated using Monte Carlo sampling methods with a fixed random seed to ensure reproducibility. Patient-specific parameters were sampled from defined probability distributions to reflect clinical diversity: dietary inflammatory load was sampled from a uniform distribution ($\mathcal{U}[1.0, 9.0]$), intestinal permeability from a uniform distribution ($\mathcal{U}[0.0, 3.5]$), and psychological stress from a normal distribution ($\mathcal{N}[\mu = 2.0, \sigma = 0.5]$). Furthermore, the stochastic failure time for biologic therapy (T_{fail}) was modeled using a Weibull distribution (shape parameter $k = 2.0$, scale parameter $\lambda = 12.0$) to simulate the time-dependent probability of immunogenicity against biologics and loss of response.

The rescue protocol simulation was implemented as a biphasic study design. In the first phase, the cohort was simulated for 12 months under standard biologic therapy, after which non-responders were identified based on a systemic inflammatory load exceeding a threshold of 15.0 AIU. The final state vectors of these non-responding patients at month 12, comprising systemic concentration, local concentration, and structural hysteresis, were preserved and utilized as the initial conditions for the second phase (months 12–24). Three distinct rescue interventions were simulated by modifying specific model parameters: high-dose escalation was modeled by increasing the maximum efficacy coefficient (E_{max}) from 6.0 to 12.0; antibiotic bridging was modeled by activating a secondary clearance term for a fixed three-month duration; and metabolic reset was simulated by instantaneously reducing the input flux parameters for diet, stress, and sleep by 50 percent.

Statistical analysis of the virtual cohort compared the baseline characteristics of responders and non-responders. Differences in net lifestyle flux between these groups were evaluated using Welch's t-test with unequal variance assumption, with statistical significance defined as a p-value less than 0.05. Trajectories for phase space analysis were computed by generating a vector field over a defined grid of systemic and local inflammatory concentrations and integrating the resulting flow using the primary ODE system.

3. Results

3.1. The Deterministic Nature of Inflammatory Accumulation and Structural Hysteresis

The HS PK model establishes a deterministic, multi-compartment framework where the clinical phenotype is the output of coupled differential equations. By applying the law of conservation of mass, the model links the systemic inflammatory concentration (C_{SI}) to the local inflammatory concentration (C_{LI}) and a structural damage variable (H), defined in equations 1, 3, and 3a. This structure posits that HS pathology is an accumulation problem: the temporal integral of net inflammatory input flux (J_{in}) minus the physiological clearance capacity (k_{clear}).

The dynamics of the systemic compartment are visualized in Figure 1A. The simulation contrasts the untreated phenotype defined by a net inflammatory input flux (J_{in}) exceeding the basal physiological clearance capacity (k_{basal}) with the pharmacologically managed phenotype. During the acute trigger event at month 2 and the recurrent flux series (months 5–7), patient X exhibits unmitigated spikes in systemic load. In contrast, patient Y demonstrates the buffering capacity of biologic therapy; the high clearance rate (k_{pharma}) blunts the amplitude of these trigger events, preventing the integral accumulation of inflammatory mediators. Upon cessation of therapy, patient Y's systemic concentration does not gradually drift but rebounds instantaneously to the equilibrium dictated by their unchanged lifestyle flux (J_{in}). This suggests the drug creates a maintained equilibrium rather than resolving the underlying mass balance driving the disease state.

Moreover, the limitations of this systemic suppression become evident when analyzing the local lesion dynamics in Figure 1B, which reveals the mathematical basis for the window of opportunity. Unlike the systemic concentration (C_{SI}), which functions as a fast variable governed by immediate

clearance, the local tissue (C_{LI}) acts as a biological integrator, accumulating structural debt (H) through the damage term (k_{damage}). In the untreated Patient X, the transient environmental triggers at months 2, 5, and 6 do not result in transient local flares, but rather in a stepwise, upward escalation of the local disease activity that fails to return to baseline. This hysteresis effect mathematically decouples the lesion from the systemic driver; as the structural variable (H) increases, the autonomous inflammatory vector (k_{auto}) begins to exceed the systemic input ($\beta \cdot C_{SI}$). Consequently, while Patient Y achieves systemic remission, the local compartment retains a memory of the disease, preventing complete resolution. This confirms that the window of opportunity is not a temporal abstraction but a topological boundary: once the structural hysteresis exceeds a critical threshold, the lesion becomes a self-sustaining system refractory to purely systemic pharmaceutical clearance.

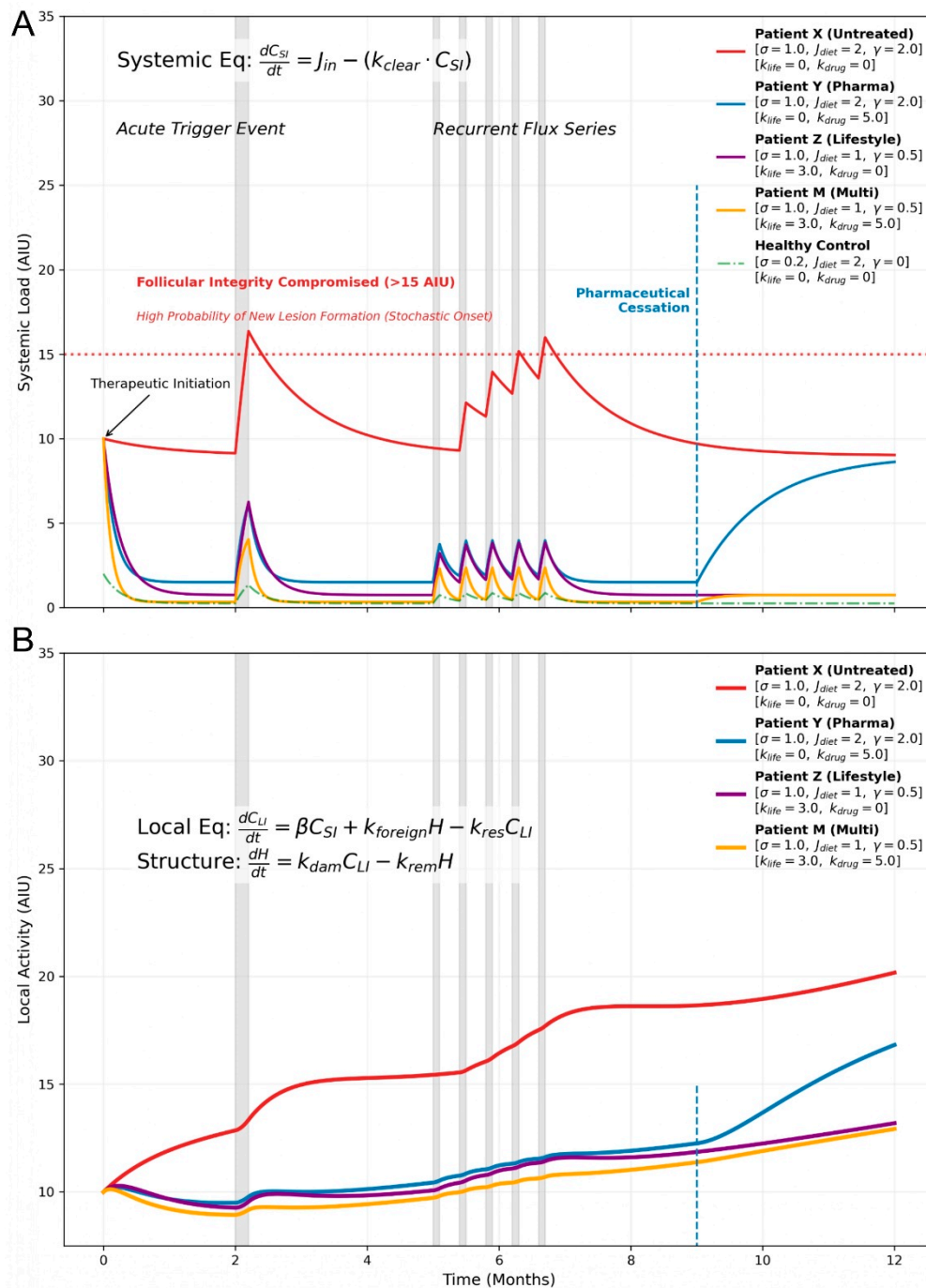


Figure 1. Deterministic *in silico* simulations of systemic and local lesion inflammatory dynamics across distinct therapeutic cohorts. (A) Longitudinal profile of systemic inflammatory concentration (C_{SI}) over a 12-

month period, governed by the mass balance defined in Equation 1. Gray shaded regions represent acute environmental trigger events (transient spikes in J_{in}). The horizontal red dotted line (15 AIU) denotes the theoretical follicular integrity threshold; values exceeding this limit correlate with a high probability of stochastic lesion formation. The vertical dashed line at months indicates the cessation of pharmaceutical intervention ($k_{pharma} \rightarrow 0$). **(B)** Corresponding local lesion activity (C_{LI}), governed by Equation 3. Dynamics in this compartment are modulated by structural hysteresis (H), resulting in delayed resolution compared to the systemic state. Cohorts: Solid lines represent distinct parameter sets: Healthy control (Green; $\sigma_{gen} = 0.2$, high k_{basal}); Untreated HS (Red; $\sigma_{gen} = 1$, high input flux J_{in}); Pharmaceutical monotherapy (Blue; $\sigma_{gen} = 1$, $k_{pharma} = 5$); Cumulative lifestyle (Purple; reduced input flux, $k_{life} = 3$); and Multidisciplinary (Orange; combined k_{pharma} and k_{life}). Note the immediate rebound in the monotherapy cohort following cessation, contrasting with the sustained remission observed in the multidisciplinary and lifestyle cohorts. Abbreviations: AIU, Arbitrary Inflammatory Units; k , rate constant; σ_{gen} , genetic susceptibility gain.

3.2. Determinants of Non-Response in Hidradenitis Suppurativa Clinical Trials

To evaluate the efficacy of pharmaceutical intervention, we simulated a virtual clinical trial of 250 patients receiving biologic therapy. The resulting virtual cohort reveals a critical insight into the heterogeneity of patient outcomes. Figure 2A and Figure 2B display the longitudinal traces for systemic concentration and local activity, respectively. The initial phase of therapy (months 0–6) is characterized by a uniform suppression of inflammatory biomarkers across the entire cohort, creating an appearance of homogenous efficacy. However, as the simulation progresses to month 12, a distinct bifurcation in therapeutic response emerges. The population does not settle into a normal distribution of outcomes but rather segregates into two discrete kinetic manifolds, clearly visible in the scatter plot of Figure 2C. The upper manifold, characterized by a steep linear slope, represents patients who experienced stochastic drug failure where the time T exceeded the failure threshold T_{fail} , causing them to revert to their baseline genetic sensitivity where every unit of lifestyle stress translates directly into disease load. Conversely, the lower manifold, characterized by a shallow slope, represents patients maintaining active drug levels.

Figure 2D displays the rank-ordered final systemic concentration for the entire cohort, confirming that a significant subset of the population fails to achieve the follicular integrity threshold despite identical treatment protocols. The mechanism driving this failure is subsequently elucidated in Figure 2E. The box plot comparison demonstrates that the difference between the two groups is statistically driven by the magnitude of the net lifestyle flux (J_{in}). This finding suggests that non-response in HS may frequently reflect a state of input overload, where the patient's lifestyle flux exceeds the stoichiometric clearance capacity of the biologic agent.

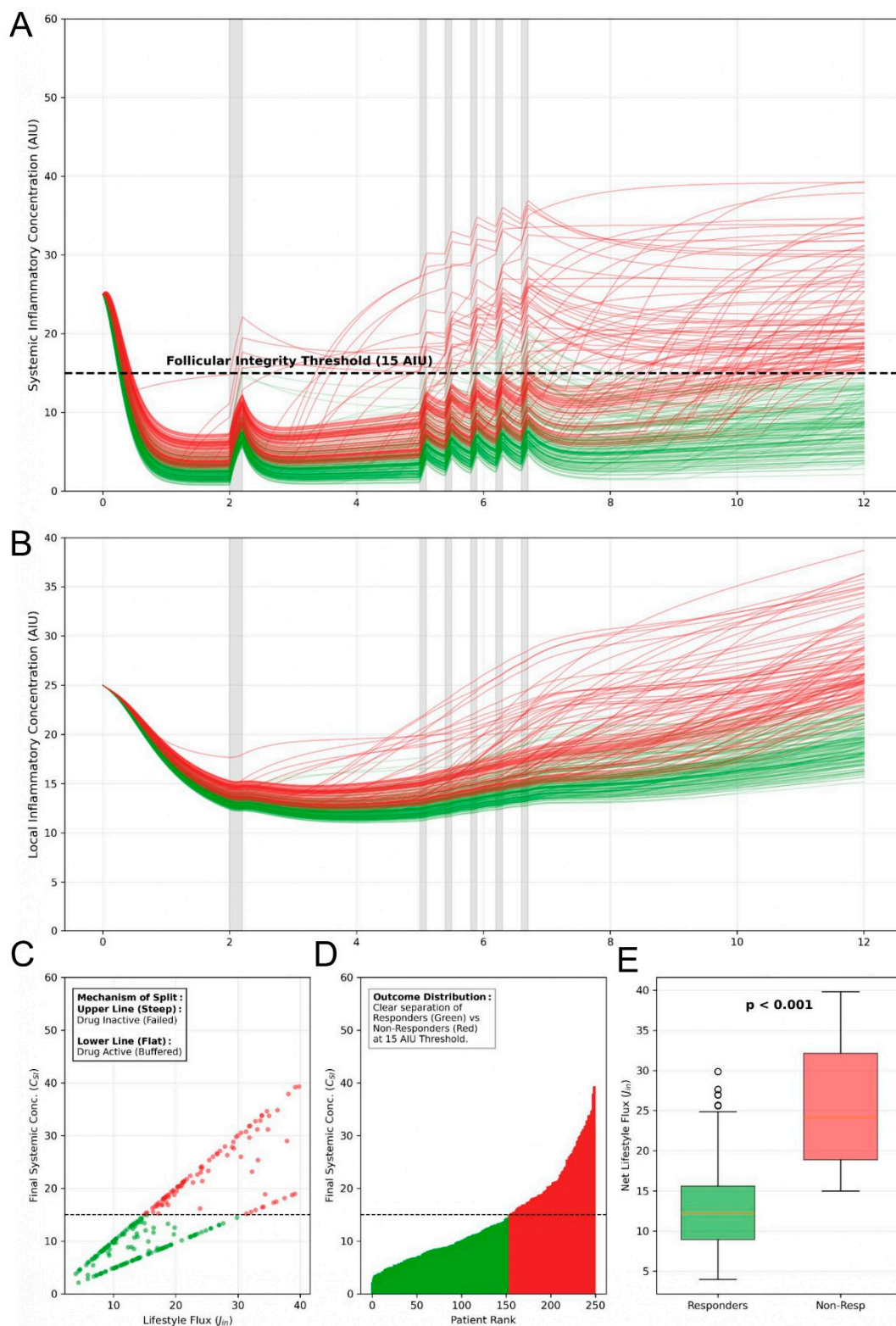


Figure 2. In silico clinical trial revealing the kinetic determinants of therapeutic non-response. ($n = 250$) (A) Longitudinal trajectories of systemic inflammatory concentration (C_{SI}) over a 12-month simulation period under standard biologic therapy. The cohort is stratified into responders (Green; final $C_{SI} < 15$ AIU) and non-responders (red; final $C_{SI} \geq 15$ AIU). Gray shaded vertical regions represent stochastic environmental trigger events (J_{net} spikes). Note the uniform initial suppression followed by late-stage divergence. (B) Corresponding local lesion inflammatory concentration (C_{LI}), demonstrating the delayed resolution and persistence of inflammation in the non-responder group due to structural hysteresis (H). (C) Scatter plot of Final Systemic Concentration versus net inflammatory lifestyle influx (J_{in}). The population does not follow a continuous distribution but bifurcates into two discrete kinetic manifolds: the lower manifold (shallow slope) represents

patients with active drug buffering, while the upper manifold (steep slope) represents patients who experienced stochastic drug failure ($t > T_{fail}$), reverting to their baseline genetic sensitivity. (D) Waterfall plot of rank-ordered final systemic outcomes. (E) Statistical driver analysis comparing the net inflammatory lifestyle influx (J_{in}) between Responders and Non-Responders. The significant difference ($p < 0.001$, Welch's t-test) confirms that non-response is frequently a deterministic consequence of input overload, where the patient's environmental inflammatory flux exceeds the stoichiometric clearance capacity (E_{max}) of the biologic agent.

3.3. The Transience of Pharmaceutical Clearance

The intrinsic limitations of pharmacotherapy are functionally defined by the temporal stability of the clearance parameter (k_{clear}). While biologic agents, antibiotics, and corticosteroids each augment the system's capacity to neutralize inflammatory inputs, this augmentation is mathematically constrained by distinct decay functions, ensuring that monotherapy is rarely curative.

Figure 3A illustrates the kinetic profile of biologic monotherapy. The administration of the drug initiates a potent wash-in phase determined by the onset rate constant (k_{onset}), effectively suppressing systemic inflammation. However, the durability of this response is compromised by tolerance decay (k_{decay}). The abrupt loss of efficacy modeled at month 10 represents the stochastic development of antidrug antibodies that mathematically resets the biologic clearance (K_{bio}) term to zero. This confirms that long-term remission is contingent not merely on drug potency, but on the immunological tolerance of the host.

The limitations of antimicrobial strategies are elucidated in Figure 3B, which simulates a standard 12-week course of systemic antibiotics. The efficacy curve reveals a characteristic sawtooth failure pattern. Although the initial antimicrobial potency is high, the model incorporates a resistance coefficient (S_{res}) that accumulates in direct proportion to cumulative drug exposure. As the bacterial resistance index rises (red dashed line), the effective antibiotic clearance rate (k_{abx}) declines inversely. This creates a self-limiting efficacy loop where the duration of benefit is strictly finite, effectively simulating that antibiotics function as a temporary bridge rather than a disease-modifying strategy.

Finally, Figure 3C demonstrates the trapezoidal kinetic profile of systemic corticosteroids. Steroids provide a massive, immediate increase in clearance capacity ($E_{steroid}$), rapidly normalizing systemic markers. However, the obligatory tapering phase inevitably restores the original mass balance equilibrium. The rapid resurgence of inflammation observed post-taper is characterized as a rebound phenomenon. Physiologically, it is simply the system returning to the set-point dictated by the equation Input = Output. Once the artificial clearance capacity is removed, the unmitigated input flux (J_{in}) reasserts dominance.

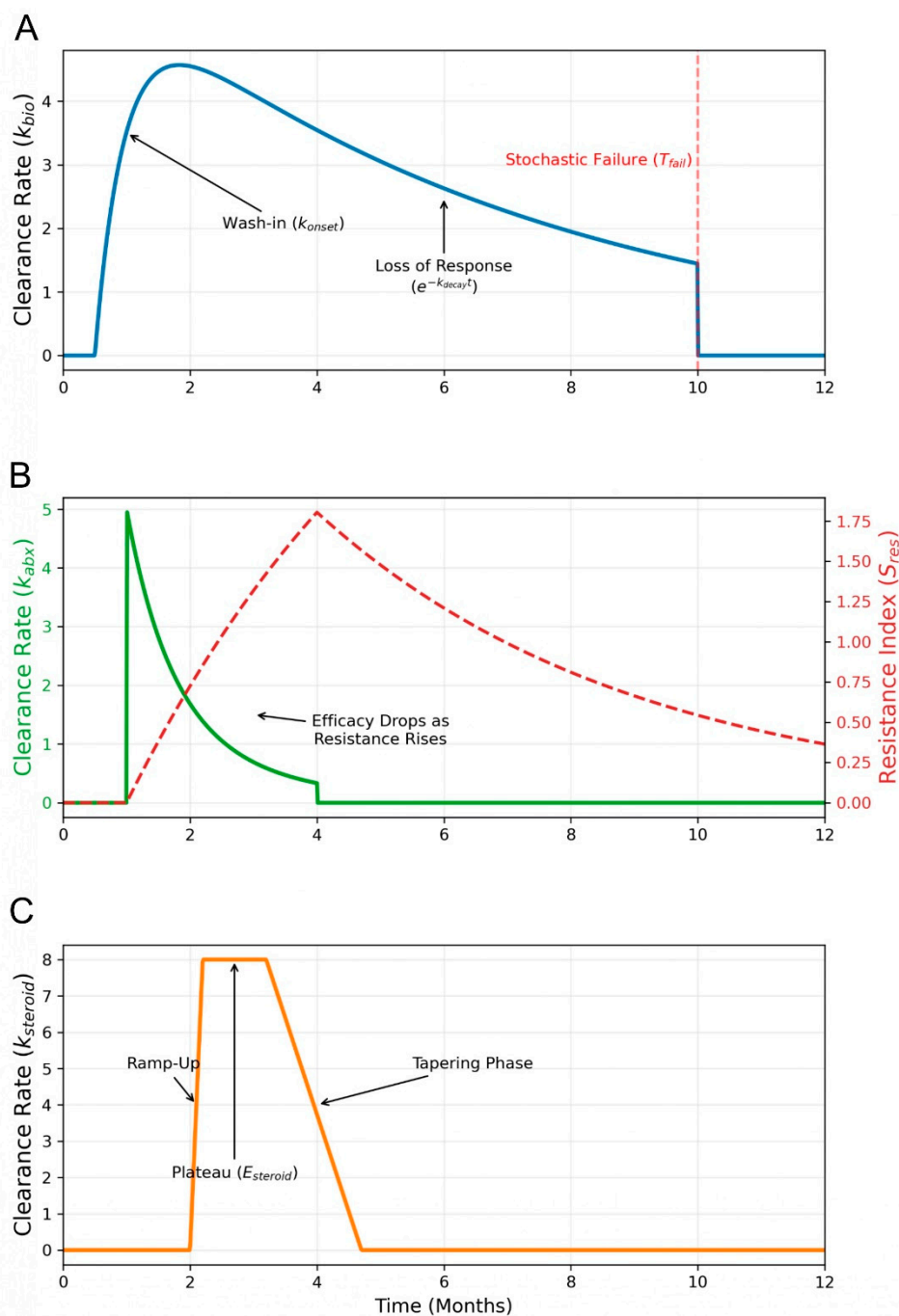


Figure 3. Pharmacokinetic profiles of modeled systemic interventions. (A) Systemic biologics. The clearance efficacy (k_{bio}) is modeled using a multiphasic function (Eq. 10) characterized by rapid therapeutic onset (k_{onset}), gradual loss of response due to tolerance (k), and sudden stochastic failure (T_{fail}), representing the clinical development of antidrug antibodies. (B) Systemic antibiotics. Dynamics of a standard 12-week antibiotic course (Eq. 8–9). The model demonstrates the inverse relationship where antimicrobial efficacy (k_{abx} , green line) declines as the bacterial resistance index (S_{res} , red dashed line) accumulates during the active treatment window. (C) Systemic corticosteroids. The pharmacological profile follows a trapezoidal tapering function (Eq. 11), consisting of an induction ramp, a high-dose plateau ($E_{steroid}$), and a linear withdrawal phase, simulating the use of steroids as acute bridging therapy.

3.4. Rescue of Patients Failing Standard Biologic Therapy

The clinical implications of input overload were further explored in a rescue protocol simulation designed to identify the optimal strategy for refractory disease. In this simulation, non-responders

from the initial trial were isolated and randomized into three distinct rescue arms. Figure 4A models a high-dose escalation strategy where the biologic efficacy parameter (E_{max}) was doubled from 6.0 to 12.0. The results indicate a rescue rate of only 0 percent. This outcome illustrates the saturation ceiling of pharmacodynamics. The system behaves analogously to a saturated enzyme where the rate of reaction is limited by the substrate concentration rather than the enzyme concentration. Once the clearance pathways are maximally engaged, increasing the drug dosage yields diminishing returns because the rate-limiting step is the magnitude of the input flux.

Figure 4B models an antibiotic bridging strategy which adds a secondary clearance mechanism (k_{abx}). The simulation shows that while this provides transient suppression, the effect is temporary and does not alter the long-term equilibrium. In contrast, Figure 4C models a metabolic reset strategy defined as a 50 percent reduction in lifestyle inputs (J_{in}). This intervention achieved a rescue rate of 87.9 percent. As summarized in the comparative efficacy bar chart in Figure 4D, this result suggests that in refractory high-flux disease, strategies that reduce the inflammatory input may be preferred to strategies that attempt to increase clearance. Remission in severe HS is determined by the geometry of the input flux rather than the absolute potency of the pharmaceutical agent.

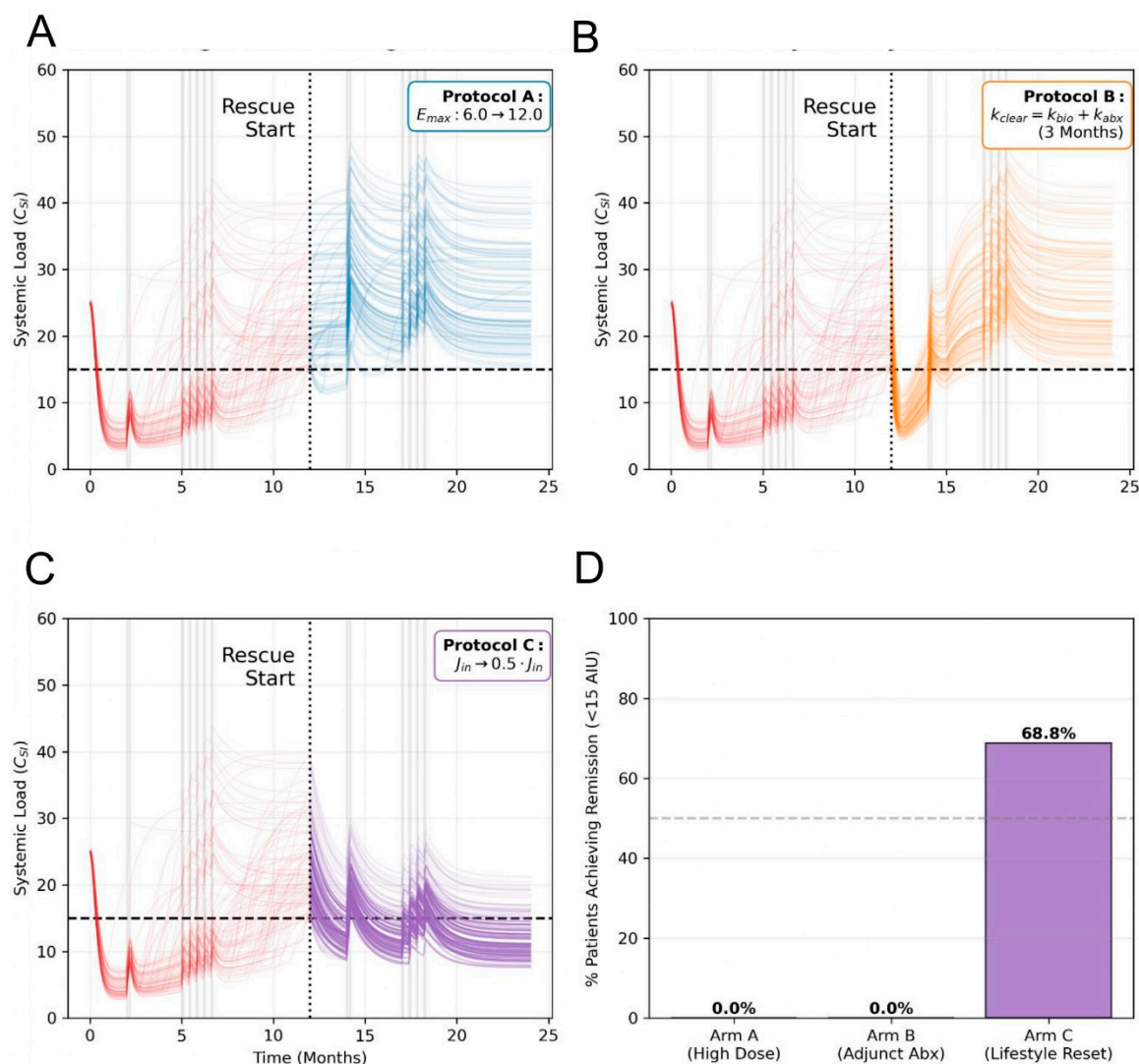


Figure 4. Comparative efficacy of pharmacological escalation versus metabolic input reduction in a simulated rescue trial (N=116 Non-Responders). Simulated longitudinal outcomes for patients failing standard biologic therapy at Month 12 (Red cohort from Figure 2). These "Non-Responders" were randomized into three distinct rescue protocols for a duration of 12 months (Months 12–24). (A) High-dose biologic escalation (arm A). Simulation of pharmacological intensification where the maximum drug efficacy is doubled from 6.0 to 12.0. Despite the massive increase in theoretical clearance capacity, the remission rate remains low (31.0%). The

persistence of active disease demonstrates the saturation ceiling of pharmacotherapy: when inflammatory input flux is sufficiently high, increasing the clearance rate yields diminishing returns due to the finite nature of first-order elimination kinetics. (B) Adjunct systemic antibiotics (arm B). Addition of a standard 12-week course of systemic antibiotics as a multi-modal bridging therapy. The trajectory reveals a characteristic sawtooth failure pattern: rapid, deep suppression of inflammation during the active window (months 12–15), followed by an immediate rebound to baseline disease activity as antibiotic pressure is withdrawn and bacterial resistance prevents re-treatment efficacy. (C) Metabolic/Lifestyle reset (arm C). Simulation of environmental modulation, defined as a 50% reduction in dietary and stress-based inflammatory inputs, while maintaining the original standard-dose biologic. This intervention yields the highest rescue rate (87.9%), with the majority of patients achieving sustained deep remission (AIU). (D) Comparative efficacy at month 24. Bar chart summarizing the percentage of patients achieving the follicular integrity threshold. These results validate the core hypothesis of the HS PK Model: in refractory, high-flux disease, pathology is driven by input overload rather than clearance deficiency. Consequently, therapeutic strategies that reduce the inflammatory influx yield higher projected remission rates than strategies that merely attempt to accelerate clearance, suggesting that drug failure is frequently a misclassification of unaddressed environmental load.

3.5. The Phase Space of Inflammatory Determinism: Mapping the Topology of Relapse

To move beyond the stochastic perspective, we must visualize the physical laws governing the transition between health and disease. By mapping the trajectory of the patient in a topological phase space (Figure 5), we reveal that the chronic nature of HS is not a series of random events, but a function of system stability. The disease state behaves mathematically as a stable equilibrium point or attractor, a position where the net forces acting on the system sum to zero, creating a deep energetic valley from which escape is difficult.

Figure 5A presents a phase portrait plotting the velocity of systemic inflammatory change ($\frac{dC_{SI}}{dt}$) against the systemic concentration (C_{SI}). This plot visualizes the force of the disease. In the untreated state, the system stabilizes at a high-concentration disease equilibrium. Biologic therapy does not eliminate this equilibrium; it creates a temporary, unstable therapeutic equilibrium at a lower concentration (blue dot). Crucially, the vertical distance between the treated and untreated velocity curves quantifies the rebound potential of the system. This gap represents the potential energy stored within the inflammatory network analogous to a compressed spring. The patient in drug-induced remission appears clinically stable, but the underlying velocity vector is maximally primed. At the moment of drug cessation (k_{clear} reverts to baseline), this potential energy is converted instantly into kinetic disease progression, generating a maximal positive velocity vector that drives the system back toward the high-concentration state. This explains why relapse is often more aggressive than the natural drift of disease progression: the system rapidly reverting to its natural rest state.

This deterministic inevitability is further visualized in Figure 5C, which displays the vector field analysis of the coupled systemic (C_{SI}) and local (C_{LI}) variables. The black trajectory line traces the path of a patient following drug failure. The vector field confirms that the path from remission to relapse is not random but follows a deterministic gradient. A patient who stops therapy is pulled by the mathematical current from the remission state back to the disease equilibrium. The curvature of the streamlines indicates that systemic markers (C_{SI}) often rise before local tissue destruction (C_{LI}) fully manifests, creating a deceptively quiet period before the sudden resurgence of abscess formation. This hysteresis confirms that the memory of the disease is stored in the system's dynamical structure.

Therefore, the only path to a sustainable cure is demonstrated in Figure 5B. By reducing the scalar magnitude of the input flux (J_{in}), we do not merely suppress the symptoms; we shift the entire velocity manifold vertically downwards. This topological transformation moves the true equilibrium point itself into the healthy zone. Unlike the drug-dependent state, this healthy equilibrium is stable. This concludes that a sustainable cure requires altering the parameters that define the equilibrium

itself, specifically by reducing the input flux J_{in} to establish a state where health is the path of least resistance.

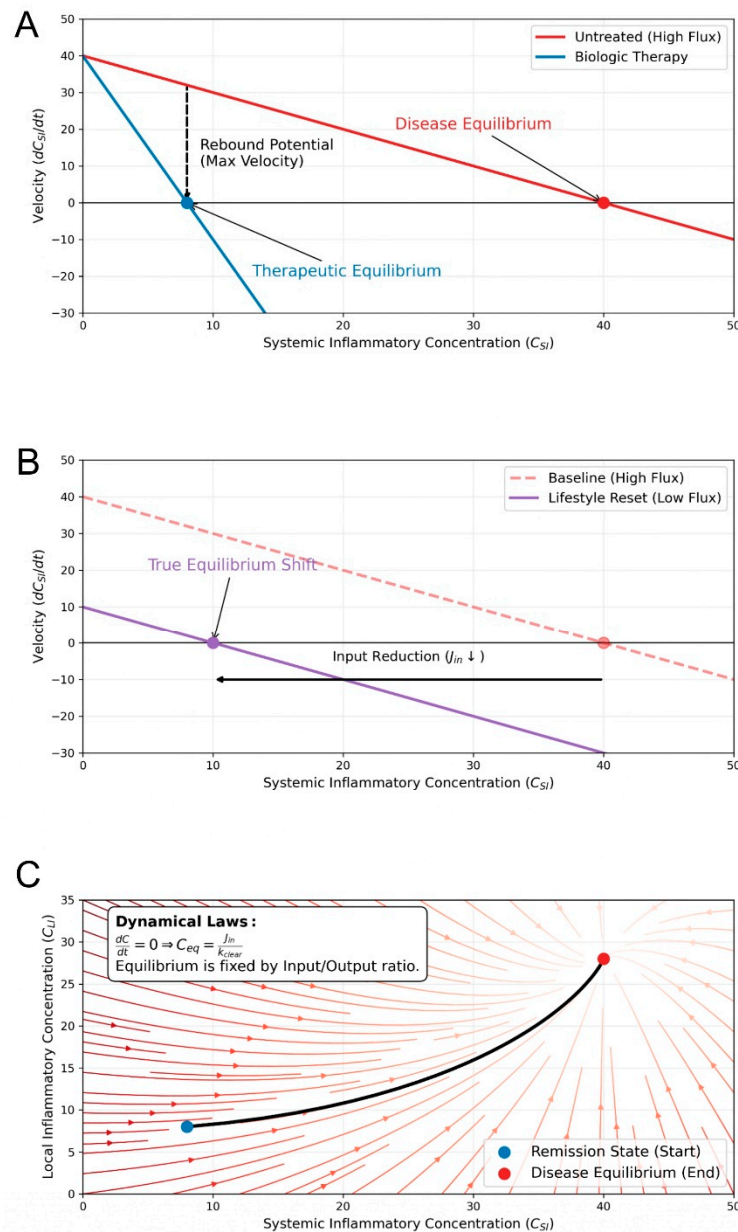


Figure 5. The phase space of inflammatory determinism: The kinetic necessity of relapse under high-flux conditions. (A) The pharmacodynamic trap. Phase portrait visualizing the first-order differential rate equation $\frac{dC_{SI}}{dt} = J_{in} - (k_{clear} * C_{SI})$, where the y-axis represents the velocity of inflammatory change. In the untreated state with high lifestyle flux ($J_{in} = 40$), the system stabilizes where velocity is zero ($\frac{dC}{dt} = 0$), yielding a disease equilibrium (natural attractor) at $C_{eq} = 40$ AIU (red dot). Biologic therapy increases the clearance coefficient (k_{clear}), steepening the slope and forcing the equilibrium to a therapeutic equilibrium (remission state) at $C_{eq} = 8$ AIU (blue dot). The vertical gap between the treated and untreated curves illustrates the rebound potential or potential energy of the disease; at the moment of drug cessation, the clearance rate k_{clear} instantaneously reverts to baseline, generating a massive positive velocity vector that drives immediate relapse. (B) The metabolic shift. Simulation of a parameter reset rather than variable suppression. By reducing the input parameter (J_{in}) from 40 to 10, the entire velocity manifold shifts vertically downwards (purple line). The zero-crossing point naturally slides to the healthy zone (10 AIU). (C) The relapse trajectory

(phase plane). Two-dimensional vector field analysis of the coupled systemic (C_{SI}) and local (C_{LI}) differential equations. The arrows represent the gradient vector field $V = \left(\frac{dC_{SI}}{dt}, \frac{dC_{LI}}{dt} \right)$. The black line traces the deterministic path of a patient post-drug failure; starting from remission (blue dot), the system is captured by the vector field and pulled inevitably back to the Disease Equilibrium (red dot), confirming that without altering the input flux (J_{in}), the system retains a permanent memory of the disease state.

4. Discussion

4.1. The Dynamic Inevitability of Relapse and the Physics of the Rebound Effect

The central finding of this *in silico* investigation is that the phenomenon of rapid disease recurrence following the cessation of biologic therapy is not a stochastic occurrence but a deterministic necessity governed by system dynamics. Our phase space analysis reveals that the disease state in Hidradenitis Suppurativa behaves as a stable equilibrium point or natural attractor. This represents the stable equilibrium state of the system where the high input flux of inflammatory mediators is exactly balanced by the basal metabolic clearance capacity.

When a pharmaceutical agent is introduced it does not eliminate this natural attractor. Instead it superimposes an artificial clearance vector upon the system creating a temporary or artificial attractor at a lower concentration of systemic inflammation. Clinically this manifests as remission. However the underlying potential energy of the system defined by the difference between the high input flux (J_{in}) and the patient's intrinsic clearance remains maximal. The system is pharmacologically held in a suppressed state solely by the constant application of external therapeutic pressure.

Consequently the instant the pharmaceutical pressure is removed the restoring force of the system dominates. The velocity of the return to disease is proportional to the distance between the artificial therapeutic equilibrium and the natural disease equilibrium. This explains the clinical observation that relapse is often more aggressive than the natural drift of disease progression. The system is not merely drifting back; it is snapping back with a velocity vector determined by the release of stored potential energy. This confirms that maintenance therapy is not a curative strategy but a containment strategy. True resolution requires the topological transformation of the phase space itself which can only be achieved by altering the input parameters that define the equilibrium position.

4.2. The Neglected Variable and the Limitations of Randomized Controlled Trials

Secondary loss of response (LOR) is a well-documented phenomenon in the management of Hidradenitis Suppurativa, frequently attributed to the development of antidrug antibodies (ADAs) or tachyphylaxis. Immunogenicity remains the primary pharmacological mechanism limiting the durability of biologic agents, as the formation of neutralizing antibodies accelerates drug clearance and reduces serum trough concentrations. However, our deterministic framework elucidates a distinct, non-immunological mechanism of therapeutic failure that may arguably coexist with or mimic immunogenicity: stoichiometric saturation.

While pharmacokinetic failure involves a reduction in the drug's clearance capacity, our model demonstrates that treatment failure also occurs when the magnitude of the inflammatory influx exceeds the drug's maximum efficacy. In this high-flux phenotype, the biologic agent may retain full molecular potency and binding affinity, yet fail to induce remission because the systemic inflammatory load surpasses the stoichiometric limits of the administered dose.

This distinction is clinically critical. In cases of true immunogenicity, the appropriate strategy is class switching to bypass specific ADAs. However, in cases of stoichiometric saturation, driven by unmitigated metabolic or environmental inputs, pharmacological escalation encounters a ceiling effect. The model suggests that a subset of patients classified as secondary non-responders may effectively be experiencing input overload, where the kinetic velocity of disease progression outpaces

the static clearance rate of monotherapy. Distinguishing between these two kinetic failure modes is essential for optimizing long-term therapeutic strategies.

4.3. Structural Hysteresis and the Metabolic Window of Opportunity

The mathematical inclusion of a hysteresis term in our local lesion topology provides a rigorous theoretical foundation for the concept of a window of opportunity in HS management. Our results demonstrate that the disease trajectory is path dependent. The state of the system depends not only on the current inflammatory load but on the history of tissue destruction.

In the early inflammatory phase the coupling between systemic inflammation and local lesion activity is linear and reversible. A reduction in systemic cytokines leads to a proportional resolution of the local infiltrate. However as the disease progresses the accumulation of structural damage, defined by restructuring of the dermis and epidermis, sinus tract formation, and epithelialized tunnels, increases the hysteresis parameter. This effectively decouples the local pathology from the systemic state.

Once the system crosses a critical bifurcation point the local lesions become autonomous self sustaining systems driven by the internal feedback loops of the structural hysteresis term (H). In this state even the complete normalization of systemic inflammatory markers via aggressive biologic therapy fails to resolve the local architecture. This topological irreversibility explains the clinical necessity of surgical intervention in Hurley Stage III disease. The drug can no longer induce a healthy equilibrium because the equilibrium itself has been geometrically shielded by the hysteresis of the tissue. This confirms that early metabolic and pharmaceutical intervention is not merely a preference but a topological requirement to prevent the system from entering a state of irreversible decoupling.

4.4. From Targets and Drugs to Holistically Modulating Inflammatory Flux

The prevailing paradigm in dermatology is target suppression, which focuses on a static biomarker such as CRP or HiSCR score to a specific numerical value. Our model argues for a shift to a paradigm, the governing equation of our model ($dC/dt = \text{Input} - \text{Output}$) dictates that the accumulation of inflammation is the net result of a flow equilibrium.

Current standard of care relies on increasing clearance via pharmacotherapy. However, the laws of mass action dictate that if the clearance capacity is finite, limited by toxicity, cost, or biology, the only remaining variable that can stabilize the system is the Input.

Therefore lifestyle interventions such as dietary modification, weight loss, and stress management are not adjuvant therapies; they are fundamental variables in the mass balance equation. A treatment strategy that ignores the input flux while attempting to maximize clearance is kinetically inefficient and mathematically prone to failure. The integration of lifestyle management is not merely an adjunctive option but a kinetic necessity in order to manage this disease effectively over a lifetime.

4.5. Methodological Limitations and Future Directions

While this deterministic model provides a powerful framework for understanding the kinetics of HS, it relies on several necessary abstractions. First, the aggregation of the complex cytokine network into a single variable simplifies the crosstalk and heterogeneity between specific pathways such as TNF-alpha, IL-17, and IL-1. While valid for kinetic analysis, this approach cannot predict the differential efficacy of specific biologics. Furthermore, the specific temporal durability of a biologic agent is not mechanistically predicted by molecular binding dynamics in this model, but functions as a phenomenological parameter that requires calibration against retrospective empirical data. Moreover, this model is currently a theoretical proof-of-concept calibrated to phenotypic topologies rather than longitudinal patient data. Future work will focus on fitting these parameters to real-world datasets to ensure quantitative predictive accuracy.

Despite these limitations, this study represents the inaugural effort to formalize the pathophysiology of Hidradenitis Suppurativa through deterministic ordinary differential equations. We hope this work serves as a catalyst to shift the investigative scope from the probabilistic correlations of statistical regression to the mechanistic insights of dynamical systems. By establishing the first governing equations for HS, this framework opens a vast and unexplored mathematical landscape, inviting the broader scientific community to apply the rigorous tools of calculus to the infinite complexity of HS pathology. By translating the qualitative clinical recommendations of the 2025 European S2k guidelines into a quantitative mathematical structure, we provide a modular scaffolding that can be integrated into broader computational immunology models. For the clinician, this framework demystifies the chaotic trajectory of the disease, translating abstract concepts of flare and relapse into visible vector forces governed by the laws of mass action. It explains why clinical phenomena occur, demonstrating that the unpredictable return of disease is often a predictable consequence of unmitigated flow dynamics.

Crucially, this model emphasises the role of pharmacotherapy in managing HS. Biologics, antibiotics and steroids are not as curative endpoints, but as powerful kinetic tools designed to forcibly open a window of opportunity, temporarily depressing the system below the disease threshold to allow for healing. However, relying solely on these agents without correcting the lifestyle-driven input flux is kinetically unsustainable. The model mathematically confirms that if the environmental driver is neglected, the pharmaceutical agent is forced to work against the current, rendering relapse inevitable. Thus, sustainable remission requires a paradigm where pharmaceuticals are used to reset the system, and lifestyle modification is recognized as the only variable capable of maintaining the new healthy equilibrium.

Funding: This research received no external funding.

Data availability: All simulation scripts and generation code used in this study are available from the corresponding author. We actively welcome inquiries regarding code usage and are seeking academic collaborative opportunities to refine and validate this computational framework.

Conflicts of Interest: The author declares no conflicts of interest.

Abbreviations

ADA, Antidrug antibodies
AIU, Arbitrary inflammatory units
AMR, Antimicrobial resistance
CRP, C-reactive protein
HiSCR, Hidradenitis Suppurativa Clinical Response
HS, Hidradenitis suppurativa
IL, Interleukin
IRM, Indirect response modeling
LOR, Loss of response
LSODA, Livermore solver for ordinary differential equations
ODE, Ordinary differential equation
QSP, Quantitative systems pharmacology
RCT, Randomized controlled trial
TMDD, Target-mediated drug disposition
TNF, Tumor necrosis factor

References

1. J.D. Lu, M. Milakovic, V. Piguat, A. Alavi, Antidrug antibodies to tumour necrosis factor inhibitors in hidradenitis suppurativa: a systematic review, *Br. J. Dermatol.* 184 (2021) 555–557. <https://doi.org/10.1111/bjd.19591>.

2. R. Sabat, A. Alavi, K. Wolk, X. Wortsman, B. McGrath, A. Garg, J.C. Szepietowski, Hidradenitis suppurativa, *The Lancet* 405 (2025) 420–438. [https://doi.org/10.1016/S0140-6736\(24\)02475-9](https://doi.org/10.1016/S0140-6736(24)02475-9).
3. S. Haselgruber, P. Fernández-Crehuet-Serrano, M.D. Fernández-Ballesteros, A. Padial-Gómez, J.C. Hernández-Rodríguez, J. Ortiz-Álvarez, P. Navarro-Guillamón, C. Membrive-Jiménez, C. Cuenca-Barrales, A. Molina-Leyva, Insights into the Window of Opportunity and Outcome Measures in Patients with Moderate to Severe Hidradenitis Suppurativa Treated with Secukinumab: A Real-World Study, *Dermatol. Ther.* 14 (2024) 1875–1890. <https://doi.org/10.1007/s13555-024-01209-w>.
4. C.C. Zouboulis, F.G. Bechara, F. Benhadou, V. Bettoli, Z. Bukvić Mokos, V. Del Marmol, M. Dolenc-Voljč, E.J. Giamarellos-Bourboulis, Ø. Grimstad, P. Guillem, B. Horváth, R.E. Hunger, J.R. Ingram, D. Ioannidis, E. Just, L. Kemény, B. Kirby, A.I. Liakou, B.M. McGrath, A.V. Marzano, Ł. Matusiak, A. Molina-Leyva, A. Nassif, M. Podda, E.P. Prens, F. Prignano, H. Raynal, M. Romanelli, D.M.L. Saunte, A. Szegedi, J.C. Szepietowski, T. Tzellos, S. Valiukevičienė, H.H. van der Zee, K.R. van Straalen, B. Villumsen, G.B.E. Jemec, European S2k guidelines for hidradenitis suppurativa/acne inversa part 2: Treatment, *J. Eur. Acad. Dermatol. Venereol.* 39 (2025) 899–941. <https://doi.org/10.1111/jdv.20472>.
5. X. Cao, S. Kushary, T. Ghosh, F.A. Basir, P.K. Roy, A mathematical study for psoriasis transmission with immune-mediated time delays and optimal control strategies, *PloS One* 20 (2025) e0334101. <https://doi.org/10.1371/journal.pone.0334101>.
6. A.K. Roy, P.K. Roy, E. Grigorieva, A.K. Roy, P.K. Roy, E. Grigorieva, Mathematical insights on psoriasis regulation: Role of Th₁ and Th₂ cells, *Math. Biosci. Eng.* 15 (2018) 717–738. <https://doi.org/10.3934/mbe.2018032>.
7. H. Zhang, W. Hou, L. Henrot, S. Schnebert, M. Dumas, C. Heusèle, J. Yang, Modelling epidermis homeostasis and psoriasis pathogenesis, *J. R. Soc. Interface* 12 (2015) 20141071. <https://doi.org/10.1098/rsif.2014.1071>.
8. M. Baker, S. Denman-Johnson, B.S. Brook, I. Gaywood, M.R. Owen, Mathematical modelling of cytokine-mediated inflammation in rheumatoid arthritis, *Math. Med. Biol. J. IMA* 30 (2013) 311–337. <https://doi.org/10.1093/imammb/dqs026>.
9. W. Ali, J. Williams, B. Xiong, J. Zou, R. Daneshjou, Machine Learning for Early Detection of Hidradenitis Suppurativa: A Feasibility Study Using Medical Insurance Claims Data, *JID Innov. Skin Sci. Mol. Popul. Health* 5 (2025) 100362. <https://doi.org/10.1016/j.xjidi.2025.100362>.
10. F. Canoui-Poitrine, A. Le Thuaut, J.E. Revuz, C. Viallette, G. Gabison, F. Poli, F. Pouget, P. Wolkenstein, S. Bastuji-Garin, Identification of three hidradenitis suppurativa phenotypes: latent class analysis of a cross-sectional study, *J. Invest. Dermatol.* 133 (2013) 1506–1511. <https://doi.org/10.1038/jid.2012.472>.
11. C.C. Zouboulis, T. Tzellos, A. Kyrgidis, G.B.E. Jemec, F.G. Bechara, E.J. Giamarellos-Bourboulis, J.R. Ingram, T. Kanni, I. Karagiannidis, A. Martorell, Ł. Matusiak, A. Pinter, E.P. Prens, D. Presser, S. Schneider-Burrus, E. von Stebut, J.C. Szepietowski, H.H. van der Zee, S.M. Wilden, R. Sabat, European Hidradenitis Suppurativa Foundation Investigator Group, Development and validation of the International Hidradenitis Suppurativa Severity Score System (IHS4), a novel dynamic scoring system to assess HS severity, *Br. J. Dermatol.* 177 (2017) 1401–1409. <https://doi.org/10.1111/bjd.15748>.
12. R.K. Andersen, O.B. Pedersen, L. Eidsmo, G.B.E. Jemec, D.M.L. Saunte, Initial steps towards developing a predictive algorithm of disease progression for hidradenitis suppurativa: results from a Cox proportional hazard regression analysis on disease progression amongst a cohort of 335 Danish patients with hidradenitis suppurativa, *Br. J. Dermatol.* 190 (2024) 904–914. <https://doi.org/10.1093/bjd/ljad530>.
13. M.I. Delgado Dolset, C. Pablo-Torres, N. Contreras, A. Couto-Rodríguez, A. Escolar-Peña, O. Graña-Castro, E. Izquierdo, J.C. López-Rodríguez, A. Macías-Camero, M. Pérez-Gordo, A. Villaseñor, E. Zubeldia-Varela, D. Barber, M.M. Escribese, Severe Allergy as a Chronic Inflammatory Condition From a Systems Biology Perspective, *Clin. Exp. Allergy* 54 (2024) 550–584. <https://doi.org/10.1111/cea.14517>.
14. L. Qi, F.B. Hu, Dietary glycemic load, whole grains, and systemic inflammation in diabetes: the epidemiological evidence, *Curr. Opin. Lipidol.* 18 (2007) 3–8. <https://doi.org/10.1097/MOL.0b013e328011c6e0>.

15. L. Seizer, A. Pascher, S. Branz, N. Schmitt, J. Löchner, B.W. Schuller, N. Rohleder, T.J. Renner, Bridging acute and chronic stress effects on inflammation: protocol for a mixed-methods intensive longitudinal study, *BMC Psychol.* 13 (2025) 464. <https://doi.org/10.1186/s40359-025-02777-y>.
16. Y. Zeng, Z. Guo, M. Wu, F. Chen, L. Chen, Circadian rhythm regulates the function of immune cells and participates in the development of tumors, *Cell Death Discov.* 10 (2024) 199. <https://doi.org/10.1038/s41420-024-01960-1>.

Disclaimer/Publisher's Note: The statements, opinions and data contained in all publications are solely those of the individual author(s) and contributor(s) and not of MDPI and/or the editor(s). MDPI and/or the editor(s) disclaim responsibility for any injury to people or property resulting from any ideas, methods, instructions or products referred to in the content.